Inhibition of Oxygen-Induced Retinopathy in RTP801-Deficient Mice

Anat Brafman,[1] Igor Mett,[1] Millicent Shafir,[1] Helen Gottlieb,[1] Golda Damari,[1] Sabrina Gozlan-Kelner,[1] Vicktoria Vishnevskia-Dai,[2] Rami Skaliter,[1] Paz Einat,[1] Alexander Faerman,[1] Elena Feinstein,[1] and Tzipora Shoshani[1]

Purpose. Ischemic proliferative retinopathy, which occurs as a complication of diabetes mellitus, prematurity, or retinal vein occlusion, is a major cause of blindness worldwide. In addition to retinal neovascularization, it involves retinal degeneration, of which apoptosis is the main cause. A prior report has described the cloning of a novel HIF-1–responsive gene, RTP801, which displays strong hypoxia-dependent upregulation in ischemic cells of neuronal origin, both in vitro and in vivo. Moreover, inducible overexpression of RTP801 promotes the apoptotic death of differentiated neuron-like PC12 cells and increases their sensitivity to ischemic injury and oxidative stress. The purpose of the study was to examine the potential role of RTP801 in the pathogenesis of retinopathy, using RTP801-deficient mice.

Methods. Wild-type and RTP801-knockout mice were used in a model of retinopathy of prematurity (ROP). Their retinas were collected at postnatal day (P)14 and P17. They were examined by fluorescein angiography and by analysis of VEGF expression, neovascularization, and apoptosis.

Results. The expression of RTP801 was induced in the wild-type retina after hypoxia treatment. The retinal expression of VEGF after transfer to normoxic conditions was similarly upregulated in both wild-type and knockout mice. Nevertheless, the retinas of the RTP801-knockout mice in an ROP model showed a significant reduction in retinal neovascularization ($P < 0.0001$) and in the number of apoptotic cells in the inner nuclear layer ($P < 0.0001$).

Conclusions. In the absence of RTP801 expression, development of retinopathy in the mouse model of ROP was significantly attenuated, thus implying an important role of RTP801 in the pathogenesis of ROP. *(Invest Ophthalmol Vis Sci.* 2004; 45:3796–3805) DOI:10.1167/iovs.04-0052

The inappropriate proliferation of retinal capillaries derived from preexisting vessels (retinal neovascularization) is a significant complication of many ocular conditions constituting the major causes of blindness. The current ability to prevent retinal neovascularization is severely limited and relies on ablation of functional retina using laser photocoagulation or cryotherapy.

Neovascularization is usually accompanied by retinal degeneration and may actually be secondary to it, because conditions of oxidative stress linked to diabetes or hyperoxygenation lead to retinal capillary damage. This results in retinal ischemia and secretion of vascular endothelial growth factor (VEGF) by astrocytes.[1] In parallel, pathologic changes of apoptotic nature occur in retinal neurons.[2]

Little is known about the actual mechanisms that induce apoptosis in retinal diseases, and none of the treatments proposed for ischemic proliferative retinopathy seem to alter the course of degeneration in the retina. A role for oxygen-derived free radicals in mediating hyperoxia-induced vaso-obliteration is supported by studies showing that the administration of exogenous antioxidants can attenuate retinopathy in certain animal models[3] and possibly in humans as well.[4] In addition, experimental oxygen-induced retinopathy is associated with the formation of lipid peroxides in the retina.[5]

Two regulatory factors worth mentioning in the context of retinopathy are p53 and hypoxia inducible factor (HIF)-1. Apoptosis induced by retinal ischemia in rats is associated with increased expression of p53 mRNA,[6] whereas mice with a reduced expression of p53 show resistance to ischemia-induced retinal ganglion cell death, confirming a functional role for this protein.[7] p53 is known to trigger the expression of several genes implicated in cellular redox control that ultimately contribute to p53-mediated apoptosis through the mitochondrial apoptotic cascade.[8,9] HIF-1 also transactivates multiple genes that play key roles in redox control and in oxygen homeostasis. Its levels are increased throughout the hypoxic inner retina, playing a role in upregulation of VEGF.[10]

We have recently reported the identification and cloning of a novel direct transcriptional target of HIF-1, RTP801.[11] Later on, RTP801 (REDD1) was demonstrated to be a shared transcriptional target of p53 and p63.[12] We detected strong upregulation of RTP801 by hypoxia both in vitro, in numerous cell lines, and in vivo, in an animal model of ischemic stroke. The gene was overexpressed, both in hypoxia-affected neurons within the penumbra region and in endothelial cells within the ischemic core, hence hinting of its potential functional role in diseases associated with these two types of cells. Inducible overexpression of RTP801 promoted the apoptotic death of differentiated neuron-like PC12 cells and drastically increased their sensitivity to ischemic injury and oxidative stress.[11] Moreover, Ellisen et al.,[12] detected that overexpression of RTP801 leads to the generation of reactive oxygen species (ROS).

Taking into account the specificities of regulation of RTP801 transcription (HIF-1 and p53 responsiveness), its expression pattern in disease (neurons and endothelial cells) and the consequences of its overexpression (increased generation of ROS and apoptosis of neuron-like cells), RTP801 seems an ideal candidate to study for involvement in retinopathy.

From [1]Quark Biotech, Inc., Fremont, California; and the [2]Department of Ophthalmology, Assaf Harofeh Medical Center, Sackler School of Medicine Tel-Aviv University, Zerifin, Israel.

Submitted for publication January 19, 2004; revised June 1, 2004; accepted June 25, 2004.

Disclosure: **A. Brafman**, Quark Biotech, Inc. (E); **I. Mett**, Quark Biotech, Inc. (E); **M. Shafir**, Quark Biotech, Inc. (E); **H. Gottlieb**, Quark Biotech, Inc. (E); **G. Damari**, Quark Biotech, Inc. (E); **S. Gozlan-Kelner**, Quark Biotech, Inc. (E); **V. Vishnevskia-Dai**, None; **R. Skaliter**, Quark Biotech, Inc. (E); **P. Einat**, Quark Biotech, Inc. (E); **A. Faerman**, Quark Biotech, Inc. (E); **E. Feinstein**, Quark Biotech, Inc. (E); **T. Shoshani**, Quark Biotech, Inc. (E).

The publication costs of this article were defrayed in part by page charge payment. This article must therefore be marked "*advertisement*" in accordance with 18 U.S.C. §1734 solely to indicate this fact.

Corresponding author: Elena Feinstein, Quark Biotech, Inc., Weizmann Science Park, POB 4071, Ness Ziona 70400, Israel; elenaf@qbi.co.il

Investigative Ophthalmology & Visual Science, October 2004, Vol. 45, No. 10

In this study, to assess the role of RTP801 in the disease's pathogenesis, we used mice with the germline disruption of RTP801 in a model of retinopathy of prematurity (ROP). The model is produced in newborn mouse pups (postnatal day [P]7) by exposure to 75% oxygen for 5 days and subsequent recovery in a room-air environment.[15] The retinal disease that develops in the model of ROP combines many features that are also characteristic of other types of retinopathy. The pathogenesis is triggered by hyperoxia-induced obliteration of vulnerable retinal blood vessels of newborn mice.[15] After the transfer of pups to the normoxic conditions (P12), the developing relative retinal hypoxia leads to secretion of angiogenic factors, such as VEGF,[15,16] and induction of abnormal vasoproliferation[10] (usually measured at P17), as well as to neuronal apoptosis occurring in the inner nuclear cell layer of the retina (maximum at P14).[2,17–19]

Our results indicated that lack of RTP801 expression significantly reduces retinal pathologic neovascularization and apoptosis in the mouse model of ROP. This points to the important role that activation of RTP801 plays in the pathogenesis of retinopathy.

Materials and Methods

Generation of RTP801-Deficient Mice

RTP801 mutant mice were generated by Lexicon Genetics Inc. (The Woodlands, TX) as a service. The RTP801 targeting vector was constructed with the Lambda KOS system previously described by Wattler et al.[20] The Lambda KOS phage library, arrayed over 96 superpools, was screened by PCR with one primer located in exon 1 of mouse RTP801 (RTP801-1; 5′- GCTGTTGTCCGCAATCTTCG-3′) and another primer located in exon 2 (RTP801-11; 5′-CACTGTTGCTGCTGTC-CAGG-3′). The PCR-positive phage superpools were plated and screened by filter hybridization with a mouse RTP801-specific probe. Two pKOS genomic clones were identified in the library screen and confirmed by sequence and restriction analysis. Gene-specific arms, (5′-CCTTAGCAGCCAGCGTCCTGGCGTCTGACG-3′) and (5′-CCCC-ATCCCCGAACCCAATTCGGCCCCGGC-3′), were appended by PCR to a yeast selection cassette containing the URA3 marker. One of the RTP801-containing genomic clones, pKOS90, and the yeast selection cassette were cotransformed into yeast. Clones that had undergone homologous recombination to replace a 212-bp region encompassing the RTP801 first coding exon (exon 2) with the yeast selection cassette were isolated. The yeast cassette was subsequently replaced with a LacZ/Neo selection cassette to complete the RTP801 targeting vector. The *Not*I linearized targeting vector was electroporated into 129/SvEv^{Tac} (Taconic) embryonic stem (ES) cells. After selection in 0.2 mg/mL of G418 for 7 to 9 days, G418/FIAU-resistant ES cell clones were isolated, and correctly targeted clones were identified and confirmed by Southern blot analysis with the 404-bp 5′ internal 52/48 probe (amplified by using PCR primers RTP801-52; 5′-CCTTGGCAGCTGCT-GAAAG-3′ and RTP801-48; 5′-GGTCAGCGAAGATTGCGGAG-3′), and the 312-bp 3′ external 49/51 probe (amplified by using PCR primers RTP801-49; 5′-AGCCATCTGCCTGCCTTGTC-3′ and RTP801-51; 5′-CCCTCACTTGGAGATTATGAC-3′). Southern blot analysis using probe 52/48 detected a 7-kb wild-type band and 5.3-kb mutant band in *Xba*I-digested genomic DNA, whereas probe 49/51 detected a 9-kb wild-type band and 7.5-kb mutant band in *Eco*RI-digested genomic DNA (not shown). Two targeted ES cell clones were microinjected into C57BL/6 (albino) blastocysts. The resultant chimeras were mated to C57BL/6 (albino) females to generate mice that were heterozygous for the RTP801 mutation.

Genotyping was performed by PCR on genomic DNA extracted from mouse tails, using two forward oligonucleotides: a neomycin-specific oligonucleotide (5′-GATGGATTGCACGCAGGTTC-3′) (Fig. 1A, primer c) and an RTP801 exon 2–specific oligonucleotide (5′-CTGG-GATCGTTTCTCGTCCTC-3′) (Fig. 1A, primer a), along with a shared RTP801 intronic reverse oligonucleotide (5′-CATCCAGGTATGAG-GAGTCTG-3′) (Fig. 1A, primer b). The PCR reactions were conducted with DNA polymerase (Super-Therm; JMR Holdings, London, UK) according to the manufacturer's protocol and simultaneously included all three primers. The reactions consisted of 30 cycles: 94°C for 45 seconds, 55°C for 2 minutes, and 72°C for 1 minute, and were completed by a 10-minute incubation at 72°C.

Rodent Model of ROP

All animal experiments were performed in strict adherence to the ARVO Statement for the Use of Animals in Ophthalmic and Vision Research and in accordance with the National Institutes of Health guidelines. Animal protocols were reviewed and approved by the Hebrew University Animal Research Committee. Oxygen-induced retinopathy was obtained in wild-type rat or mouse (C57BL6/129) pups or in RTP801-knockout mouse pups according to a protocol previously established for the mouse model of ROP.[13] In brief, at P7, rodent pups and their nursing mothers were exposed to hyperoxic conditions (75% oxygen) for 5 days in an infant incubator (Ohmeda Medical, Louisville, CO). On P12, the pups were returned to room-air (normoxic) conditions for 2 or 5 days until P14 or P17, respectively. Age-matched animals were maintained in room air (normoxic conditions) for the duration of the experiment.

Retinal Angiography and Quantification of the Avascular Area

Fluorescein angiography of the retina was performed as described previously.[21] On P17, wild-type and RTP801-knockout mice, either control or exposed to relative hypoxic conditions, were deeply anesthetized and perfused through the left ventricle with 1 mL of 50 mg/mL fluorescein-labeled high molecular weight (2,000,000) dextran (Sigma-Aldrich, St. Louis, MO) in PBS. The mice were killed and their eyes were enucleated. One eye of each mouse was fixed in 10% formalin for 10 minutes. The retinas were separated from the sclera, the retinal pigment epithelium, the lens, and the cornea and fixed for an additional 2 hours. Then, each retina was cut at four to five peripheral locations and flatmounted on a glass slide in PBS-glycerol. The flatmounted retinas were photographed under a fluorescence microscope (MZFLIII; Leica, Deerfield, IL; digital camera Spot RT color; Diagnostics Instruments, Inc., Sterling Heights, MI). The capillary-free area was quantified from the digital images in masked fashion (Photoshop; Adobe, Mountain View, CA).

Assessment of Retinal Neovascularization Response

Mouse eyes that were not used for angiography were fixed in 10% formalin, embedded in paraffin, and sectioned. Quantification of the neovascular response was performed in 7-μm-thick sagittal sections, 140 μm apart from each other and spanning the entire retina. After staining with periodic acid-Schiff (PAS) reagent and hematoxylin, the extent of neovascularization was determined by counting neovascular cell nuclei anterior to the internal limiting membrane (at the vitreous side). Eyes of 9 to 10 mice from each genotype/treatment group were analyzed. For each eye, 9 to 13 retinal sections were evaluated in a fully masked protocol, and the mean number of neovascular nuclei per section was determined.

Assessment of Apoptosis In Vivo

The same sectioning procedure that was used for the assessment of the neovascularization response was also used for the quantification of apoptotic cells. Apoptosis was detected in retinas of P14 and P17 mice by terminal deoxynucleotidyltransferase-mediated dUTP-biotin nick end labeling (TUNEL). The assay was performed with a peroxidase in situ apoptosis detection kit (ApopTag; Intergen, Purchase, NY) according to the manufacturer's protocol. The sections were counterstained with methyl-green, and seven to eight mice from each genotype/

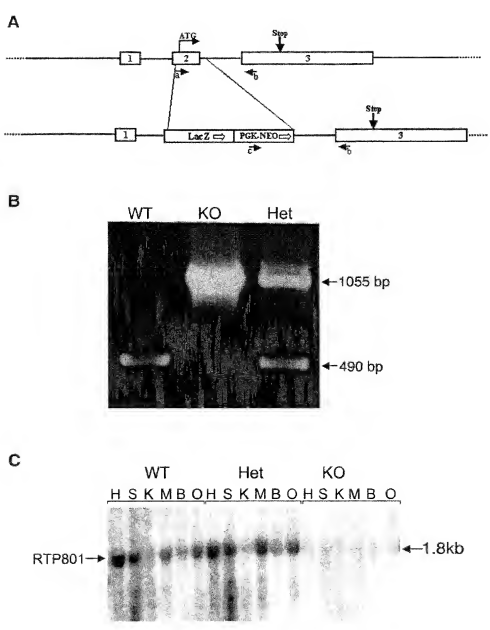

FIGURE 1. Generation of RTP801-deficient mice. (A) Schematic representation of targeted replacement of RTP801 exon 2 with the LacZ/neo expression cassette. (B) Identification of mouse genotype by PCR analysis of tail-derived genomic DNA. PCR products were analyzed on 1% agarose gel. The WT allele was detected as 490-bp band, whereas the targeted knockout (KO) allele was detected as a 10,550-bp band. Both alleles were detected in heterozygous (Het) animals. (C) Northern blot analysis of mRNA isolated from heart (H), spleen (S), kidney (K), muscle (M), brain (B), and ovary (O) of wild-type, heterozygous, or knockout mice, hybridized to RTP801-specific cDNA probe.

treatment group were evaluated. For each eye, 10 to 19 sections were counted in a masked protocol and the mean number of TUNEL-positive nuclei in the retinal inner nuclear layer (INL) was determined. Some of the slides were also stained with hematoxylin-eosin to confirm apoptosis by morphologic characteristics.

Statistical Analysis of Morphometric Data

Because the parameters of interest were assessed in the biological material obtained in several different experimental sets, the analysis was performed by ANOVA, using factorial models (models of contrasts) to abolish the influence of interexperimental differences. The models were generated separately for evaluation of each specific parameter (neovascularization, or apoptosis).

In Situ Hybridization

Eyes from relative hypoxia-treated and control rodent pups were excised on either day P14 or P17, fixed in 10% formalin, sliced, and used for in situ hybridization with ^{35}S-UTP labeled rat RTP801-specific and VEGF-A–specific sense and antisense riboprobes. Radioactive riboprobes were produced from a vector (pBluescript; Stratagene, LaJolla, CA) containing ratRTP801 cDNA encompassing the whole open reading frame of the gene, using either T7 (antisense probe) or T3 (sense probe) polymerases, as previously described.[22] In situ hybridization was performed according to a previously published protocol.[23] The exposed slides were developed (D-19 developer; Eastman Kodak, Rochester, NY), fixed, and counterstained with hematoxylin-eosin. The microphotographs were taken using a microscope (Axioscop-2; Carl Zeiss Meditec, Dublin, CA) equipped with a charge-coupled device (CCD) camera (Spot RT; Diagnostic Instruments).

RNA Extraction from Paraffin-Embedded Mouse Eyes

RNA from formalin-fixed, paraffin-embedded mouse eyes was extracted according to a previously published protocol.[24] The excess of paraffin around the fixed eyes was carefully removed, and the whole samples were cut into 5-μm sections. Some of the samples had been

partially sectioned previously, and therefore the amount of sections obtained per eye varied ranging from a maximum of 400 to a minimum of 200. Every 100 freshly cut eye sections were positioned into one screw-cap tube (Eppendorf, Fremont, CA), and paraffin was extracted twice by short vortexing and incubation for 10 minutes with 1 mL xylene at room temperature. The samples were next washed twice with 100% ethanol, dried briefly on air, and resuspended in 0.5 mL lysis buffer (10 mM NaCl, 0.5 M Tris-HCl [pH 7.6], 20 mM EDTA, 1% SDs, and 0.5 mg/mL proteinase K) and incubated at 45°C overnight with shaking. RNA was extracted once with an equal volume of phenol-chloroform-isoamyl alcohol (25:24:1) and twice with chloroform-isoamyl alcohol (24:1). RNA was precipitated with an equal volume of isopropanol with an addition of linear polyacrylamide as a carrier. Each RNA pellet was washed twice with 70% ethanol. All RNA pellets obtained from the same eye were combined and dissolved in 15 μL double-distilled sterile water per 100 sections.

Quantification of RTP801 and VEGF Expression in the Retina

Relative amounts of RTP801 and VEGF-A mRNAs and that of a control gene (rhodopsin) were quantified by real-time PCR analysis (LightCycler system; Roche Diagnostics, Indianapolis, IN). Of each RNA sample extracted from paraffin-embedded mouse eyes, 3.5 μL was reverse transcribed in a 20-μL reaction mixture containing 0.33 nM random hexamer primers (Roche Diagnostics) with reverse transcriptase (Superscript II; Invitrogen, San Diego, CA) and the supplied enzyme buffer. RNA and the primer were preannealed at 72°C for 2 minutes and then combined with the remaining reaction components on ice. Reverse transcription (RT) was performed at 25°C for 10 minutes and at 42°C for 1 hour and was terminated by heating at 95°C for 5 minutes. Each RT reaction was diluted 1:25 and 1:50 in double-distilled water, and 2.5 μL of each dilution was added to 7.5 μL of a reaction mix (LightCycler FastStart DNA Master SYBR Green I; Roche Diagnostics), containing 5 pM of PCR amplification primer pairs (final concentration). All runs were performed in duplicate. The reactions were run with the following parameters: denaturation at 95°C for 7 minutes and 35 amplification cycles (95°C for 10 seconds, 55°C for 5 seconds, and 72°C for 8 seconds). Relative standard curves were generated for each primer set so that the input amount from the samples could be calculated. The following PCR primers were used for amplification: mouse RTP801, 5′-GCCGGAGGAAGACTCTCAT-3′ and 5′-GCTGCATCAGGTTGGCACAC-3′; mouse VEGFA, 5′-GCAGGCTGCTGTAACGATGAA-3′ and 5′-TCCGCATGATCTGCATGGTGA-3′; and mouse rhodopsin, 5′-TTGCCACACTTGGAGGTGAA-3′ and 5′- ACCACCACGTAGCGGTCAAT-3′. Each primer pair was verified to generate a single specific amplified DNA fragment, and each RNA sample was verified to yield no PCR bands in the absence of reverse transcriptase, thus excluding DNA contamination. Because in situ hybridization analysis detected RTP801 and VEGF induction exclusively in the retinas and because some of the paraffin blocks were partially sectioned, we included a rhodopsin-specific PCR reaction as a normalization control. In addition, the results were normalized to the initial RNA concentrations.

Results

Generation of RTP801-Deficient Mice

To investigate the role of RTP801 in various pathologic conditions, we established a mouse strain with a germline disruption of RTP801. As illustrated in Figure 1A, the targeting vector was designed to replace the second exon, containing the initiation ATG, of RTP801 with the LacZ/neomycin resistance cassette. The targeting vector was linearized and electroporated into LEX-1 ES cells. Two cell clones containing the disrupted RTP801 allele were identified and injected into C57BL/6 blastocysts to generate chimeric mice. Germline transmission of the mutant allele was obtained. Genotyping was performed by PCR analysis with template DNA from tail biopsy specimens (Fig. 1B). Expression deficiency of RTP801 was confirmed by Northern blot analysis with a full-length RTP801 cDNA probe (Fig. 1C). As opposed to the wild-type mice, no RTP801 expression was detected in any of the tissues tested in the knockout mice (heart, spleen, kidney, muscle, brain, and ovary).

The absence of RTP801 had no obvious consequences for prenatal and postnatal development and growth of the mice. Mice homozygous for the RTP801 deletion were born normal, and the mutant allele was transmitted in a Mendelian manner. They were weaned at the same age as the wild-type mice, had body weights and physical features indistinguishable from normal, and were normally fertile. General morphologic examination and histologic assessment of retinas, specifically, did not reveal any pathologic changes.

Expression of RTP801 in the Model of ROP

Before the functional assessment of the role that RTP801 may play in ROP, we studied whether the gene's expression is specifically induced in this model. In situ hybridization analysis with an RTP801-specific antisense riboprobe was performed on retinal sections from P14 mouse (not shown) and rat (Figs. 2A–D) pups either subjected to ROP or grown under normal conditions. Sections of control normoxic retina displayed a very weak background hybridization signal in all retinal layers (Fig. 2B). RTP801-specific hybridization signal was significantly elevated in hypoxic retinas, with the maximum concentration in the outer portion of the INL (Figs. 2C, 2D). The sense probes gave no hybridization signal (not shown). To further substantiate our findings, we performed a quantitative real-time RT-PCR with mouse RTP801-specific primers and RNA extracted from formalin-fixed, paraffin-embedded wild-type mouse eyes enucleated on P14 from the treated and control pups. This quantitative analysis confirmed the in situ hybridization results (Fig. 2E). Thus, we concluded that RTP801 is upregulated in hypoxic retinal cells in the model of perinatal retinopathy both in rats and mice.

Retinal Vaso-obliteration and Neovascularization in the ROP Model in RTP801-Deficient Mice

To determine the role that RTP801 plays in the pathogenesis of retinopathy, wild-type and RTP801-knockout mice were subjected to the model of ROP.[15] Simultaneous availability of wild-type and knockout age-matched litters was assured by establishment of mating between mice heterozygous for the RTP801 null allele. The structure of the retinal blood vessel tree was initially evaluated in fluorescein-injected flatmounted retinas at 5 days after the transfer of mice from hyperoxic to normoxic conditions (P17). The representative retinal images are shown in Figure 3. As is evident, the vascular network of wild-type mice in the model of ROP was significantly altered compared with the vascular network of control mice grown in normoxic conditions. These alterations were typical of retinas that have undergone vaso-obliteration[15] and were expressed in central vasoconstriction and in a severe loss of central retinal microvasculature (Figs. 3C, 3E). Because the analysis was performed on P17, the hypoxic retinas of wild-type mice also displayed the features indicative for a strong ongoing vasoproliferative response: vessel tortuosity (Fig. 3C) and blood vessel tufts (Fig. 3E). In marked contrast, the retinal vascular tree of RTP801-knockout mice subjected to the model of ROP looked significantly less affected (Figs. 3D, 3F). However, the signs of central vaso-obliteration and of neovascularization response were still present (compare Fig. 3D with 3B). Retinal angio-

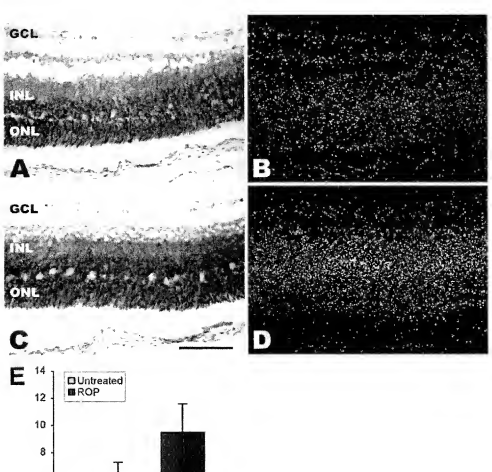

FIGURE 2. In situ hybridization analysis of RTP801 expression in the rat model of perinatal retinopathy (P14). Representative bright-field (**A**, **C**; hematoxylin-eosin staining) and parallel dark-field (**B**, **D**) images of retinal histologic sections derived from rat pups grown in normoxic conditions (**A**, **B**) and from pups in the ROP model (**C**, **D**). GCL, ganglion cell layer; INL, inner nuclear cell layer; ONL, outer nuclear cell layer. The sections were hybridized in situ to RTP801 riboprobe. The hybridization signal was evident as *black dots* in the bright-field images and as *white dots* in the dark-field images. Scale bar, 100 μm. (**E**) Relative normalized amounts of RTP801 RNA quantified by real-time PCR in the retinas of five control and six treated wild-type mouse pups. $P = 0.004$ (two-tailed, equal variances *t*-test).

grams of control age-matched wild-type and knockout mice kept in normoxic conditions were indistinguishable from each other (Figs. 3A, 3B). The quantitative comparison of the nonperfused retinal areas (using angiographic image analysis as previously described[25]) between wild-type and knockout mice revealed a statistically significant reduction in the latter genotype ($P = 0.04$, one-tailed *t*-test; Fig. 3G).

For quantitative assessment of the vasoproliferation response, we embarked on counting the nuclei of endothelial cells in the new blood vessels extending into the vitreous beyond the internal limiting membrane.[13] The nuclei were observed in PAS/hematoxylin-stained retinal sections (Fig. 4A) and an average of 230 sections for each genotype/treatment group were assessed. No neovascular nuclei were found in retinas of either wild-type or RTP801-knockout mice grown in normoxic conditions, whereas both wild-type and knockout retinas showed a neovascular response in the ROP model. However, there was a significant difference ($P < 0.0001$) between the number of retinal neovascular nuclei in the wild-type and RTP801-deficient mice (Fig. 4B). Whereas the average number of neovascular nuclei in hypoxic wild-type retinas was 43, the average number of nuclei counted in retinas of similarly treated RTP801-null mice was only 16. Thus, the absence of RTP801 expression in the model of ROP significantly attenuated the neovascularization response.

Neuroretinal Apoptosis in RTP801-Deficient Mice in the Model of ROP

Occurrence of TUNEL-positive cells in the INL of retinas of wild-type and RTP801-knockout mice grown in room air or in the ROP model, was estimated at days P14 and P17. At P14, both groups of room-air–raised control mice had a similar ($P = 0.8$) low number of TUNEL-positive cells in the INL (Fig. 5B). When assessed at P14 after exposure to ROP model, both wild-type and knockout mice had a significantly elevated number of apoptotic INL cells ($P < 0.0001$ and $P = 0.015$, respectively). However, the average numbers of TUNEL-positive cells in the knockout mice were significantly reduced ($P < 0.0001$) compared to the wild-type ones: 16 vs. 28 (Figs. 5). The INL TUNEL-positive cells exhibited typical signs of apoptosis, including pericentric clumps of chromatin, pyknotic nuclei, and cosinophilic cytoplasm, thus supporting the apoptotic nature of the DNA breaks detected by the TUNEL technique (Fig. 5A). At P17, the number of INL TUNEL-positive cells in both wild-type and RTP801-knockout mice in the ROP model was significantly reduced and approximated the corresponding numbers detected in the control animals at P14 ($P = 0.15$ and $P = 0.65$, respectively; Fig. 5B). Thus, we concluded that the absence of RTP801 expression in the model of ROP significantly attenu-

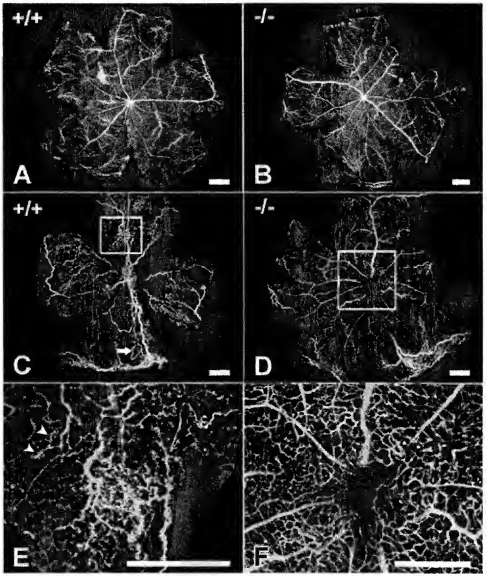

FIGURE 3. Retinal vascular network of wild-type and RTP801-knockout mice subjected to the model of ROP. Representative images of flat-mounted fluorescein-perfused P17 retinas from wild-type (A, C, E) (+/+) and RTP801 knockout (−/−) mouse pups (B, D, F). The retinas shown in (A) and (B) were derived from pups grown in normoxic conditions, whereas retinas shown in (C) and (D) were from pups in the ROP model. *Boxed* areas in (C) and (D) are shown at higher magnification in (E) and (F), respectively. Signs of neovascularization are shown: tortuous blood vessels (C, *arrow*) and neovascular tufts (E, *arrowheads*). Scale bar, 0.5 mm. (G) Percentage of capillary-free area from the total retinal area, as quantified in four wild-type and three knockout mouse pups in the ROP model. $P = 0.04$ (one-tailed, unequal variances *t*-test).

ated the hypoxia-induced apoptotic response of the INL cells.

Expression of VEGF in Wild-Type and RTP801-Deficient Mice in the ROP Model

We next investigated the retinal expression of VEGF-A by in situ hybridization in wild-type and RTP801-knockout mice in the ROP model. Despite the observed differences between the genotypes in their neovascularization response, the expression of VEGF mRNA was upregulated in P17 retinas of ROP-subjected mice, regardless of their genotype (Fig. 6A). Similar VEGF upregulation was also observed at P14 in both wild-type and knockout retinas, as detected by both in situ hybridization analysis (not shown) and by quantitative real-time PCR (Fig.

6B). These results indicate that the mode of VEGF expression did not substantially differ between wild-type and RTP801-knockout mice.

Discussion

In ocular diseases such as diabetic retinopathy, ROP, and retinal arterial or vein occlusions, hypoxic conditions developing as a consequence of vascular occlusion often lead to pathologic angiogenesis and neuroretina degeneration,[17,26,27] which in some cases cause severe visual loss.

Our data demonstrate that RTP801, a novel HIF-1–responsive gene,[11] is not only upregulated in the INL in the rodent model of ROP but also functionally contributes to the development of retinal disease in this model. RTP801-knockout mice in the model of ROP clearly demonstrated a significant attenuation in the development of major pathologic features usually documented for this model: retinal vaso-obliteration, retinal neovascularization, and apoptosis of INL cells. Because of the complexity of ROP pathogenesis and the mutual influence and

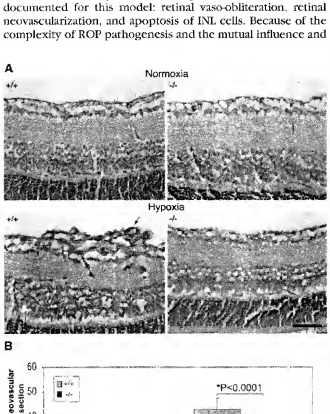

FIGURE 4. Analysis of retinal neovascularization in mice in the model of ROP (P17). (A) Representative PAS-stained histologic sections of retinas derived from wild-type (+/+) or RTP801-knockout (−/−) mice either grown in normal conditions (normoxia) or exposed to relative hypoxia during ROP model (hypoxia). *Bottom left, arrow:* new blood vessels growing beyond the inner limiting membrane. Scale bar, 50 μm. (B) Average number (per section) of extra retinal neovascular nuclei in PAS-stained retinal sections derived from wild-type or RTP801-knockout mice in the model of ROP. The analysis was performed on day P17. The results were obtained in two independent experiments.

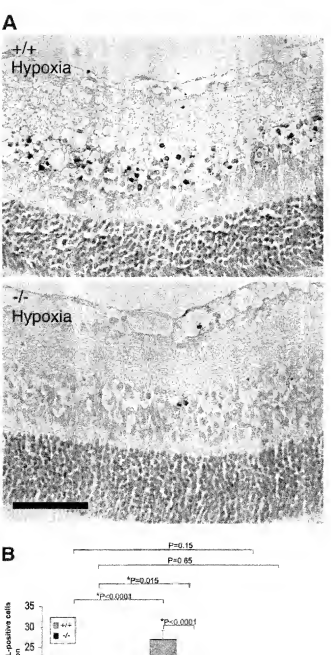

FIGURE 5. Analysis of apoptosis in the central retina on P14. (A) Representative images of TUNEL-stained central retinal sections obtained from wild-type (+/+) or RTP801 knockout (−/−) mice exposed to relative hypoxia in the course of ROP model. Scale bar, 50 μm. (B) Average number (per section) of TUNEL-stained cells in the INL of retinas derived from wild-type or RTP801-knockout mice grown either in normal conditions (P14-N) or exposed to relative hypoxia (P14-H and P17-H). The results were obtained in three independent experiments.

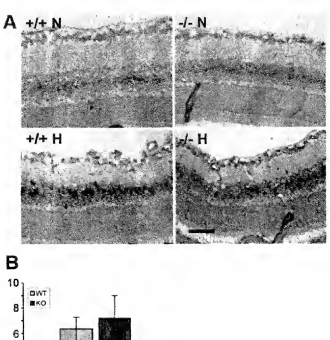

FIGURE 6. VEGF expression in the retinas of RTP801 knockout and wild-type mice in the model of ROP. (A) Bright-field images of retinal sections derived from wild-type (−/+) and RTP801 knockout (−/−) mice, either grown in normal air conditions (N; normoxia) or in the model of ROP (H; hypoxia) and analyzed at P17. Retinal sections were hybridized in situ to a VEGF-A–specific riboprobe. The hybridization signal was evident as *black dots*. Scale bar, 50 μm. (B) Relative normalized amounts of VEGF-A RNA at P14 quantified by real-time PCR in the retinas of seven control and five treated wild-type mouse pups in the ROP model. $P = 0.18$ (two-tailed, two samples equal variance *t*-test).

interconnection of its different stages, at present it is difficult to pinpoint the primary event that is affected by the absence of RTP801. Previous studies[11,12] have demonstrated that overexpression of RTP801 may lead to apoptosis in target cells. It is conceivable that a lack of RTP801 may protect endothelial cells (notably, induction of RTP801 expression in the endothelial cells, e.g., within a poststroke necrotic zone, has been reported[11]) from hyperoxia-induced apoptosis resulting in reduced retinal vaso-obliteration. This, in turn, may lead to a lesser subsequent relative hypoxia after transfer to normal air. Lesser hypoxia may lead to the reduction of compensatory VEGF secretion and neovascularization and of apoptosis occurring in the INL during the hypoxic stage of retinopathy.[25]

However, this view may indeed be too simplistic, as in reality the mechanism of protective effect of RTP801 deficiency appears to be more complex, reflecting its direct involvement at all the stages of the pathogenesis. First, it seems that whereas there was a clear direct correlation between the size of nonperfused retinal area and the number of neovascular nuclei in the wild-type mice, this correlation was not so obvious in the RTP801 knockout animals (Fig. 7), indicating that relationships between these two pathologic processes may be perturbed in the absence of RTP801. Second, significant reduction of vasoproliferative response in the knockout mice was not accompanied by a significant reduction in retinal VEGF expression, as confirmed by both in situ hybridization and quantitative RT-PCR analyses. It is important to indicate, however, that although VEGF is considered a major factor triggering neovascularization in the hypoxic retina,[18,28] it acts together with other factors, being by itself insufficient to induce retinal neovascularization.[2] Expression of some of these factors may be influenced by RTP801, and it will be interesting to identify them in the future. Third, the absence of RTP801 may directly prevent the occurrence of neuroretinal apoptosis in the hypoxic phase of ROP rather than the protection from apoptosis being secondary to the overall reduced vascular retinal disease. This view is supported by a substantial amount of data. Thus, we have previously demonstrated that overexpression of RTP801 in differentiated neuron-like PC12 cells promotes their apoptotic death and sensitization to hypoxic conditions in vitro.[11] Moreover, it was recently found that the expression of antisense RTP801 RNA protected neuroblastoma cells from amyloid-β toxicity.[29] Finally, our preliminary data indicate that primary cortical neurons from RTP801-knockout mice are twice as resistant as control cells in conditions of oxidative stress created by hydrogen peroxide treatment in vitro.

The specific molecular mechanism by which the absence of RTP801 expression attenuates retinal disease in the model of ROP remains unknown. RTP801 has been shown to modulate cellular ROS levels and cell sensitivity to oxidative stress.[11,12] Excessive formation of reactive oxygen intermediates is strongly implicated in the pathogenesis of ROP,[30] affecting both blood vessel integrity and neuronal survival. The administration of antioxidants to mice exposed to a hyperoxia regimen attenuated the development of retinopathy.[31] Thus, it is tempting to speculate that RTP801 may be functionally involved in these processes.

The identification of RTP801, as a downstream target of both p53 and HIF-1,[11,12] suggests that it may function in concert with other redox regulatory genes, known to be induced by these two transcription factors. Both p53 and HIF-1 were shown to be involved in oxygen-induced retinopathy and to constitute an important part of the control of neovascularization.[6,32] A recent study indicates that in hypoxic conditions, HIF-1α regulates p53 activity at the levels of stability and nuclear export through interactions with Mdm2.[33] Furthermore, in hypoxic neurons HIF-1α and p53 conspire to promote a pathologic sequence resulting in cell death.[34] The direct

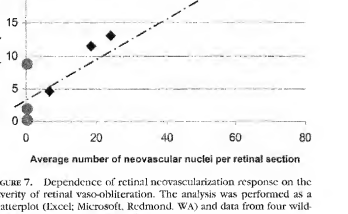

FIGURE 7. Dependence of retinal neovascularization response on the severity of retinal vaso-obliteration. The analysis was performed as a scatterplot (Excel; Microsoft, Redmond, WA) and data from four wild-type (WT) and three knockout (KO) mice in the ROP model, for which both parameters (average number of neovascular nuclei per section [Fig. 4] and percent of capillary-free area [Fig. 4]) were available. WT: correlation = 0.94; KO: correlation = −1.56575E-16.

transcriptional control of RTP801 by both p53 and HIF-1 stresses that both pathways involved in redox regulation merge at a certain stage.

Many pathologic features developing in the rodent model of ROP are common in a more frequent type of proliferative retinopathy, diabetic retinopathy. These include ROS-induced vaso-obliteration, reactive neovascularization, and neuronal apoptosis in the INL.[35,36] Suppression or attenuation of ischemic proliferative retinopathy would be a highly effective therapeutic option for many retinal disorders. The current treatment of proliferative retinopathies is panretinal laser photocoagulation, which in many cases is effective but not optimal. In addition to possible recurrence and progression of the disease, requiring repeated laser treatments, there are also significant side effects, which include the loss of peripheral and night vision. Several experimental alternative approaches have been designed to curtail the development and/or progression of retinal neovascularization. These approaches include targeting growth factors,[18,37] cell surface receptors,[38] or proteinases.[39] Our studies demonstrate that RTP801 may be regarded as a novel therapeutic target for treatment of proliferative retinopathies. Inhibition of RTP801 function may lead to the attenuation of both vasoproliferation and neurodegeneration symptoms. Currently, several VEGF-inhibiting drugs are being developed for the treatment of retinal diseases.[40,41] Because the lack of RTP801 seems to attenuate retinopathy without influencing VEGF production (at least in the model of ROP), whereas a certain residual retinal disease is still present in the knockout mice, simultaneous targeting of both genes may yield a more profound synergistic therapeutic effect. The potential use of RTP801 as a drug target for the treatment of ischemic proliferative retinopathy thus warrants further study.

Acknowledgments

The authors thank Leonid Brodsky for help with statistical analyses, Lexicon Genetics Incorporated for generation of knockout mice.

References

1. D'Amore P. Mechanisms of retinal and choroidal neovascularization. *Invest Ophthalmol Vis Sci.* 1994;35:3974–3979.
2. Morita M, Ohneda O, Yamashita T, et al. HLF/HIF-2alpha is a key factor in retinopathy of prematurity in association with erythropoietin. *EMBO J.* 2003;22:1134–1146.
3. Niesman MR, Johnson KA, Penn JS. Therapeutic effect of liposomal superoxide dismutase in an animal model of retinopathy of prematurity. *Neurochem Res.* 1997;22:597–605.
4. Kretzer FL, Mehta RS, Johnson AT, Hunter DG, Brown ES, Hittner HM. Vitamin E protects against retinopathy of prematurity through action on spindle cells. *Nature.* 1984;309:793–795.
5. Penn JS. Oxygen-induced retinopathy in the rat: possible contribution of peroxidation reactions. *Doc Ophthalmol.* 1990;74:179–186.
6. Joo CK, Choi JS, Ko HW, et al. Necrosis and apoptosis after retinal ischemia: involvement of NMDA-mediated excitotoxicity and p53. *Invest Ophthalmol Vis Sci.* 1999;40:713–720.
7. Li Y, Schlamp CL, Poulsen GL, Jackson MW, Griep AE, Nickells RW. p53 regulates apoptotic retinal ganglion cell death induced by N-methyl-D-aspartate. *Mol Vis.* 2002;8:341–350.
8. Li PF, Dietz R, von Harsdorf R. p53 regulates mitochondrial membrane potential through reactive oxygen species and induces cytochrome c-independent apoptosis blocked by Bcl-2. *EMBO J.* 1999;18:6027–6036.
9. Polyak K, Xia Y, Zweier JL, Kinzler KW, Vogelstein B. A model for p53-induced apoptosis. *Nature.* 1997;389:300–305.
10. Ozaki H, Yu AY, Della N, et al. Hypoxia inducible factor-1alpha is increased in ischemic retina: temporal and spatial correlation with VEGF expression. *Invest Ophthalmol Vis Sci.* 1999;40:182–189
11. Shoshani T, Faerman A, Mett I, et al. Identification of a novel hypoxia-inducible factor 1-responsive gene, RTP801, involved in apoptosis. *Mol Cell Biol.* 2002;22:2283–2293.
12. Ellisen LW, Ramsayer KD, Johannessen CM, et al. REDD1, a developmentally regulated transcriptional target of p63 and p53, links p63 to regulation of reactive oxygen species. *Mol Cell.* 2002;10:995–1005.
13. Smith LE, Wesolowski E, McLellan A, et al. Oxygen-induced retinopathy in the mouse. *Invest Ophthalmol Vis Sci.* 1994;35:101–111.
14. Alon T, Hemo I, Itin A, Pe'er J, Stone J, Keshet E. Vascular endothelial growth factor acts as a survival factor for newly formed retinal vessels and has implications for retinopathy of prematurity. *Nat Med.* 1995;1:1024–1028.
15. Pierce EA, Avery RL, Foley ED, Aiello LP, Smith LEH. Vascular endothelial growth factor/vascular permeability factor expression in a mouse model of retinal neovascularization. *Proc Natl Acad Sci USA.* 1995;92:905–909.
16. Gerber HP, Condorelli F, Park J, Ferrara N. Differential transcriptional revulation of the two vascular endothelial growth factor receptor genes. Flt-1, but not Flk-1/KDR, is upregulated by hypoxia. *J Biol Chem.* 1997;272:23659–23667.
17. Sennlaub F, Courtois Y, Goureau O. Inducible nitric oxide synthase mediates retinal apoptosis in ischemic proliferative retinopathy. *J Neurosci.* 2002;22:3987–3993.
18. Aiello LP, Pierce EA, Foley ED, et al. Suppression of retinal neovascularization in vivo by inhibition of vascular endothelial growth factor (VEGF) using soluble VEGF-receptor chimeric proteins. *Proc Natl Acad Sci USA.* 1995;92:10457–10461.
19. Dembinska O, Rojas LM, Varma DR, Chemtob S, Lachapelle P. Graded contribution of retinal maturation to the development of oxygen- induced retinopathy in rats. *Invest Ophthalmol Vis Sci.* 2001;42:1111–1118.
20. Wattler S, Kelly M, Nehls M. Construction of gene targeting vectors from lambda KOS genomic libraries. *Biotechniques.* 1999;26:1150–1156, 1158, 1160.
21. D'Amato R, Wesolowski E, Smith LE. Microscopic visualization of the retina by angiography with high- molecular-weight fluorescein-labeled dextrans in the mouse. *Microvasc Res.* 1993;46:135–142.
22. Komarova EA, Christov K, Faerman AI, Gudkov AV. Different impact of p53 and p21 on the radiation response of mouse tissues. *Oncogene.* 2000;19:3791–3798.
23. Faerman A, Shani M. Transgenic mice: production and analysis of expression. *Methods Cell Biol.* 1997;52:373–403.
24. Korbler T, Grskovic M, Dominis M, Antica M. A simple method for RNA isolation from formalin-fixed and paraffin-embedded lymphatic tissues. *Exp Mol Pathol.* 2003;74:336–340.
25. Miyamoto N, Mandai M, Takagi H, et al. Contrasting effect of estrogen on VEGF induction under different oxygen status and its role in murine ROP. *Invest Ophthalmol Vis Sci.* 2002;43:2007–2014.
26. Patz A. Clinical and experimental studies on retinal neovascularization. XXXIX Edward Jackson Memorial Lecture. *Am J Ophthalmol.* 1982;94:715–743.
27. Bressler NM, Bressler SB, Graqoudas ES. In: Albert DA, Jakobiec FA, eds. *Principles and Practice of Ophthalmology.* Philadelphia: WB Saunders; 1993:834–852.
28. Seo MS, Kwak N, Ozaki H, et al. Dramatic inhibition of retinal and choroidal neovascularization by oral administration of a kinase inhibitor. *Am J Pathol.* 1999;154:1743–1753.
29. Kim J-R, Lee S-R, Chung HJ, et al. Identification of amyloid β-peptide responsive genes by cDNA microarray technology: Involvement of RTP801 in amyloid β-peptide toxicity. *Exp Mol Medicine.* 2003;35:403–411.
30. Kuroki M, Voest EE, Amano S, et al. Reactive oxygen intermediates increase vascular endothelial growth factor expression in vitro and in vivo. *J Clin Invest.* 1996;98:1667–1675.
31. Penn JS, Tolman BL, Bullard LE. Effect of a water-soluble vitamin E analog, trolox C, on retinal vascular development in an animal model of retinopathy of prematurity. *Free Radic Biol Med.* 1997;22:977–984.

32. Rosenbaum DM, Rosenbaum PS, Gupta H, et al. The role of the p53 protein in the selective vulnerability of the inner retina to transient ischemia. *Invest Ophthalmol Vis Sci*. 1998;39:2132–2139.
33. Chen D, Li M, Luo J, Gu W. Direct Interactions between HIF-1alpha and Mdm2 modulate p53 function. *J Biol Chem*. 2003;278:13595–13598.
34. Halterman MW, Miller CC, Federoff HJ. Hypoxia-inducible factor-1alpha mediates hypoxia-induced delayed neuronal death that involves p53. *J Neurosci*. 1999;19:6818–6824.
35. Bek T. Transretinal histopathological changes in capillary-free areas of diabetic retinopathy. *Acta Ophthalmol (Copenh)*. 1994;72:409–415.
36. Barber A, Lieth E, Khin S, Antonetti D, Buchanan A, Gardner T. Neural apoptosis in the retina during experimental and human diabetes: early onset and effect of insulin. *J Clin Invest*. 1998;102:783–791.
37. Adamis AP, Shima DT, Tolentino MJ, et al. Inhibition of vascular endothelial growth factor prevents retinal ischemia-associated iris neovascularization in a nonhuman primate. *Arch Ophthalmol*. 1996;114:66–71.52.
38. Friedlander M, Theesfeld CL, Sugita M, et al. Involvement of integrins alpha v beta 3 and alpha v beta 5 in ocular neovascular diseases. *Proc Natl Acad Sci USA*. 1996;93:9764–9769.
39. Penn JS, Rajaratnam VS, Collier RJ, Clark AF. The effect of an angiostatic steroid on neovascularization in a rat model of retinopathy of prematurity. 2001;42:283–290.
40. Eyetech Study Group. Preclinical and phase 1A clinical evaluation of an anti-VEGF pegylated aptamer (EYE001) for the treatment of exudative age-related macular degeneration. *Retina*. 2002;22:143–152.
41. Tolantino MJ, Brucker AJ, Fosnot J, et al. Intravitreal injection of vascular endothelial growth factor small interfering RNA inhibits growth and leakage in nonhuman primate laser-induced model of choroidal neovascularization. *Retina*. 2004;24:132–138.